

The Arf-like GTPase Arl8 Mediates Delivery of Endocytosed Macromolecules to Lysosomes in *Caenorhabditis elegans*

Isei Nakae,^{*†} Tomoko Fujino,^{*†} Tetsuo Kobayashi,^{*†} Ayaka Sasaki,^{*}
Yorifumi Kikko,^{*} Masamitsu Fukuyama,^{*} Keiko Gengyo-Ando,^{‡§||}
Shohei Mitani,^{‡§} Kenji Kontani,^{*} and Toshiaki Katada^{*}

^{*}Department of Physiological Chemistry, Graduate School of Pharmaceutical Sciences, University of Tokyo, Bunkyo-ku, Tokyo 113-0033, Japan; [‡]Department of Physiology, Tokyo Women's Medical University, School of Medicine, Shinjuku-ku, Tokyo 162-8666, Japan; and [§]CREST, JST, Kawaguchi, Saitama, Japan

Submitted December 7, 2009; Revised April 19, 2010; Accepted May 12, 2010
Monitoring Editor: Sandra Lemmon

Late endocytic organelles including lysosomes are highly dynamic acidic organelles. Late endosomes and lysosomes directly fuse for content mixing to form hybrid organelles, from which lysosomes are reformed. It is not fully understood how these processes are regulated and maintained. Here we show that the *Caenorhabditis elegans* ARL-8 GTPase is localized primarily to lysosomes and involved in late endosome-lysosome fusion in the macrophage-like coelomocytes. Loss of *arl-8* results in an increase in the number of late endosomal/lysosomal compartments, which are smaller than wild type. In *arl-8* mutants, late endosomal compartments containing endocytosed macromolecules fail to fuse with lysosomal compartments enriched in the aspartic protease ASP-1. Furthermore, loss of *arl-8* strongly suppresses formation of enlarged late endosome-lysosome hybrid organelles caused by mutations of *cup-5*, which is the orthologue of human mucolipin-1. These findings suggest that ARL-8 mediates delivery of endocytosed macromolecules to lysosomes by facilitating late endosome-lysosome fusion.

INTRODUCTION

The late endosomal-lysosomal system is composed of dynamic acidic organelles that repeatedly undergo fusion and fission (Storrie and Desjardins, 1996; Mullins and Bonifacino, 2001; Luzio *et al.*, 2007). Late endosomes fuse with lysosomes transiently or completely, allowing their content to mix; thereby endocytosed macromolecules are degraded by various lysosomal hydrolases. The complete fusion between late endosomes and lysosomes creates hybrid organelles, from which lysosomes can be reformed via fission (Bright *et al.*, 1997, 2005; Pryor *et al.*, 2000). The fusion/fission events in late endosomal-lysosomal system also mediate the delivery of newly synthesized lysosomal proteins from the *trans*-Golgi network (TGN) to lysosomes via late endosomes (Luzio *et al.*, 2003). Although it is clear that the fusion/fission must be judiciously regulated to maintain the normal late endosomal-lysosomal system, the molecular mechanisms that regulate the processes are poorly understood.

Many steps of membrane traffic such as budding, transport, and fusion are regulated by small GTPases of the Rab and Arf families (Zerial and McBride, 2001; Kahn *et al.*, 2005; Gillingham and Munro, 2007; Stenmark, 2009). Among more than 60 and 20 members of Rab and Arf families, respectively, in mam-

mals, Arl8 is the first small GTPase reported to be primarily localized to lysosomes with some colocalization with late endosomal markers (Bagshaw *et al.*, 2006; Hofmann and Munro, 2006). Arl8 is highly conserved among multicellular animals, but not in the yeast *Saccharomyces cerevisiae* (Okai *et al.*, 2004). Recent reports have shown that overexpression of Arl8 affects lysosome motility in mammalian cells (Bagshaw *et al.*, 2006; Hofmann and Munro, 2006); however, the physiological function of Arl8 in the late endosomal-lysosomal system remains uncertain.

In the present study, we performed the genetic and cell biological analysis of an *arl-8* mutant using *C. elegans* and show that ARL-8 is involved in late endosome-lysosome fusion. Loss-of-function of ARL-8 gave rise to supernumerary late endosomal and lysosomal compartments, which were smaller than wild type. Formation of the supernumerary compartments in *arl-8* mutants was largely reduced by blocking early-to-late endocytic traffic. Endocytosed macromolecules were transported to late endosomal compartments in *arl-8* mutants; however, the compartments failed to fuse with lysosomal compartments enriched in the aspartic protease ASP-1. Furthermore, *arl-8* functions upstream to *cup-5*: loss-of-function of ARL-8 strongly suppressed the enlargement of late endosome-lysosome hybrid organelles caused by mutations of *cup-5*, the *C. elegans* orthologue of human mucolipin-1. On the basis of these findings, we propose that ARL-8 mediates delivery of endocytosed macromolecules to lysosomes by facilitating late endosome-lysosome fusion.

MATERIALS AND METHODS

Strains and Genetics

Worm cultures and genetic crosses were basically performed according to standard protocols (Brenner, 1974). *C. elegans* strains used in this study are listed in Supplemental Figure S8. The strains were maintained at 15 or 20°C.

This article was published online ahead of print in *MBoC in Press* (<http://www.molbiolcell.org/cgi/doi/10.1091/mbc.E09-12-1010>) on May 19, 2010.

[†] These authors contributed equally to this work.

^{||} Present address: Saitama University Brain Science Institute, 255 Shimo-Okubo, Sakura-ku, Saitama 338-8570, Japan.

Address correspondence to: Kenji Kontani (kontani@mol.f.u-tokyo.ac.jp).

Isolation of *arl-8(tm2504)*

The allele *arl-8(tm2504)* was isolated by the TMP/UV method (Gengyo-Ando and Mitani, 2000). The PCR primer sets used in the screening are: external sets, Y57G11C#F10[CTCGACTGGATTTCGCAGTCT] and Y57G11C#R7[ATTAGGCTGCAATGCTAGAG]; internal sets, Y57G11C#F11[CTTTAGAGCGCCCAATTCAC] and Y57G11C#R8[CATCCACAGTGAAGCTAC]. The isolated strain was outcrossed four times to the wild-type N2 strain and maintained over the balancer chromosome *nT1[qIs51]*. The homozygous *arl-8(tm2504)* mutant was distinguished from the heterozygote on the basis of no green fluorescent protein (GFP) fluorescence (*nT1[qIs51]*) of pharynx when scoring phenotypes.

Plasmid Constructs and Transgenic Strains

To construct pYB101 (*arl-8::GFP*, translational C-terminal GFP fusion), a DNA fragment containing the *arl-8* promoter region and the entire exon/intron without a stop codon (1.7 kb) was amplified by PCR with primers KK-388[GAAATAAGCTTGTGCTGAGAGT] and KK-406[CGGGATCCGCGTTGAGCTTTCAGTGA] and cloned into *C. elegans* GFP vector pPD95.77 (a generous gift from A. Fire, Stanford University School of Medicine). To analyze the subcellular localization of ARL-8 in coelomocytes, pYB109 (*punc-122::arl-8::mCherry*) was constructed as follows: A DNA fragment of mCherry was cloned into NotI/BglII site of an expression vector controlled by *unc-122* promoter (pFX-*unc-122p*; Gengyo-Ando *et al.*, 2006) and then a DNA fragment containing the entire exon/intron of *arl-8* without a stop codon was cloned into NotI site of the same vector. NotI site in front of the first ATG of the resultant vector was removed by PCR with primers IN-9[TTGGCTATGGTGAATAAGGTTCTCGACT] and IN-8[CATATTGTGAGCCCAATGAAGTAAAATTTTC]. To construct pYB102 (*arl-8/WT*), a DNA fragment containing *arl-8* promoter region, the entire exon/intron and 3' untranslated region (UTR; 2.3 kb) was amplified by PCR with primers KK-388 and TF-18[GGATCCCTGTACAATCACAATTCA] and cloned into pGEM-T Easy vector. pYB104 (*arl-8/T34N*) and pYB105 (*arl-8/Q75L*) were made by PCR with primers TF-1[GGAAAAACACATTTGTCAATGGTTATGCT]/TF-2[AGAGTTTGGAGCCCAACAAG] and TF-15[GATATCGGGGCGCTTCACCG]/TF-16[CCATAATTGATCGTACCGTTGCC] using pYB102 (*arl-8/WT*) as a template DNA, respectively. To construct pYB107 (*parl-8::human Arl8a*) and pYB108 (*parl-8::human Arl8b*), human cDNA fragments of Arl8a and Arl8b without the first ATG and stop codon were amplified by PCR with primers TF-35[ATCGCTTTGTTCAACAAGCTGGTCTG]/TF-36[GCTTCTCGGTGACTTCGAGT] and TF-33[CTGGCGTCACTCCCGCT]/TF-34[GCTTCTTCTAGATTTGAATGCTGAATAA], respectively. The cDNA fragment was ligated to the DNA fragment amplified by PCR with primers TF-38[TAACACTAGGCCAATCCACGACT] and TF-37[CATCTTGAATATTGATGTGAATGAGGAA] using pYB102 as a template to make a modified version of pYB102 lacking *arl-8* coding region. To express ARL-8::mCherry under heat-shock promoter control, a DNA fragment coding ARL-8::mCherry was amplified by PCR with primers KK-642[GCGGTACCATGTTGGCTATGGTGAATAAGG] and KK-643[GCGGTACCTTACTTGTACAGCTCGTCCA] using pYB109 as a template and cloned into KpnI site of pPD49.78 and pPD49.83 (generous gifts from A. Fire). To express ASP-1::DsRed, a DNA fragment was amplified by PCR with primers Y39B6#F11[TTGGTACCAGAAATTCAGCCTTCTGTATG] and Y39B6#R1[TTGGCGCCGACAAATCCCTTGTGGACGGCGG], and cloned into KpnI/NotI site of the expression vector pFX-DsRedX1 (Gengyo-Ando *et al.*, 2006). pYB116 (*punc-122::asp-1::mCherry*) was constructed as follows: a DNA fragment containing the entire exon/intron of *asp-1* without a stop codon was amplified by PCR with primers IN-94[GCGGCCGATGCAGACCTTCGTTTGTCTCG]/IN-95[GCGGCCGACAAATCCCTTGTGGACGGCG]. The DNA fragment was then cloned into NotI site of pFX-*unc-122p* containing mCherry cDNA. pYB117 (*sand-1* RNAi construct) was generated by cloning the DNA fragment of *sand-1* into the BglII/PstI sites of vector pPD129.36. A *sand-1* DNA fragment was amplified by PCR with primers IN-116[GAAGATCTGATTCATCTTCGTGATTGAAC]/IN-117[ATTGGCTGCAGGCTGACATACAGACTTGC]. To express ARL-8 under heat-shock promoter control, a DNA fragment containing the entire exon/intron of *arl-8* was amplified by PCR with primers KK-642[GCGGTACATGTTGGCTATGGTGAATAAGG] and IN-83[GGGGTACCTTAGCGTTGAGCTTTCGAGT] using N2 genomic DNA as a template and cloned into the KpnI site of pPD49.78 and pPD49.83. We performed germline transformation experiments by injecting various constructs with coinjection markers (Mello *et al.*, 1991). See also Supplemental Figure S8 for strains and plasmids used in this study.

Endocytosis Assays In Vivo

The traffic of Texas-Red and Alexa488-conjugated bovine serum albumin (TR-BSA and Alexa488-BSA, Invitrogen, Carlsbad, CA) in coelomocytes was monitored as described previously (Zhang *et al.*, 2001). TR-BSA or Alexa488-BSA (1 mg/ml in water) was injected into the body cavity of adult worms and incubated at 15 or 20°C. At the indicated times, worms were subjected to microscopic analysis. For each time point, similar results were obtained with more than five coelomocytes of different worms.

Heat-Shock Rescue Experiments

To evaluate rescue of lysosomal morphologies or endocytic traffic in *arl-8(tm2504)* mutant coelomocytes, we maintained the transgenic animals

(YB1143 or YB1306) at 15°C, shifted the adult animals from 15 to 33°C, incubated them for 30 min, and allowed them to recover at 20°C for the indicated time before scoring.

Microscopy

Animals were mounted on 3% agarose pads with 50 mM Na₂S₂O₃ in M9. Differential interference contrast (Nomarski) and fluorescent images were obtained with a Zeiss Axio Imager M1 microscope system equipped with the Axiovision software (Thornwood, NY). Confocal images were acquired with Nikon Eclipse TE2000-E (Melville, NY) equipped with Confocal scanner unit CSU10 (Yokogawa, Tokyo, Japan)/iXon DV887 (Andor, South Windsor, CT) and processed with Andor iQ, Nikon NIS-Elements, and Adobe Photoshop (San Jose, CA) software.

In Vitro Culture of Coelomocytes and Time-Lapse Confocal Microscopic Analysis

Worms were dissected using 30-gauge needles in a culture medium (137 mM NaCl, 5 mM KCl, 1 mM MgCl₂, 2 mM CaCl₂, 10 mM HEPES, 5 mM glucose, 2 mM L-asparagine, 0.5 mM L-cysteine, 2 mM L-glutamine, 0.5 mM L-methionine, 1.6 mM L-tyrosine, 26 mM sucrose; Espelt *et al.*, 2005) or CO₂-independent medium with glutamine (Invitrogen) to release coelomocytes from the pseudocoeloms. The isolated coelomocytes were incubated in 150 μl of medium containing Alexa488-conjugated BSA (10 μg/ml) or Cascade Blue dextran (20 μg/ml) in a collagen-type I (Cellmatrix type I-P, Nitta Gelatin, Tokyo, Japan) coated glass-base dish with grid (Iwaki, Holliston, MA) for 5–10 min at room temperature (~25°C). After washing four times with ice-cold medium, time-lapse fluorescence images were acquired at room temperature using a TCS-SP5 (Leica Microsystems, Deerfield, IL) equipped with a HCX PL APO 100×/1.46 NA oil objective lens. Laser lines at 405, 488, and 561 nm were used for excitation of Cascade Blue, Alexa488/GFP, and Alexa594/DsRed, respectively. Laser power was attenuated to 1.5–2% of maximum to minimize phototoxicity and photobleaching. To prepare figures, single frames were processed with Adobe Photoshop software.

Production of Anti-ARL-8 Antibody and Immunoblotting

Anti-ARL-8 antibodies were prepared in rabbits against a synthetic peptide (CDITLQWLIDHSKAQR, corresponding to the C-terminus of ARL-8) conjugated with keyhole limpet hemocyanin and purified from whole serum with the peptide-immobilized affinity column (Pierce, Rockford, IL) according to the manufacturer's instructions. Immunoblotting was performed as described previously (Saito *et al.*, 2002; Kajiho *et al.*, 2003).

RNA Interference Experiments

Feeding RNA interference (RNAi) was performed as described previously (Kamath *et al.*, 2001; Poteryaev *et al.*, 2007). In brief, adult worms (P0) were placed on either control (pPD129.36) or *sand-1* (pYB117) RNAi plates and removed after 12–24 h. After further incubation for 72 h, F1 worms were transferred to another RNAi plates seeded with the same bacteria. The coelomocyte phenotype was observed in the F2 generation. The worms were maintained at 20°C during RNAi treatment.

RESULTS

ARL-8 Is Broadly Expressed in *C. elegans*

Mammals have two closely related Arl8 homologues, Arl8a and Arl8b, whereas *C. elegans* has only one Arl8 (*arl-8*, Y57G11C.13; Li *et al.*, 2004). We made transgenic animals expressing C-terminally GFP-tagged ARL-8 under the control of the *arl-8* promoter. Figure 1, A–C, shows that ARL-8::GFP was widely expressed in many tissues including neurons, muscle, intestine, and coelomocytes in adult worms. Expression of the ARL-8::GFP fusion proteins could rescue the maternal embryonic lethality and coelomocyte phenotypes of *arl-8* mutants (Supplemental Figure S1), suggesting that the GFP fusion proteins are functional and are likely to reflect localization of endogenous ARL-8.

ARL-8 Localizes Primarily to Lysosomes in *C. elegans* Coelomocytes

ARL-8::GFP labeled the subsets of intracellular compartments in *C. elegans* coelomocytes (Figure 1C). These cells are macrophage-like scavenger cells that contain many membrane-bound compartments of different sizes and possess high endocytic and degradation activities (Grant and Sato, 2006; Fares and Greenwald, 2001a). To define the subcellular localiza-

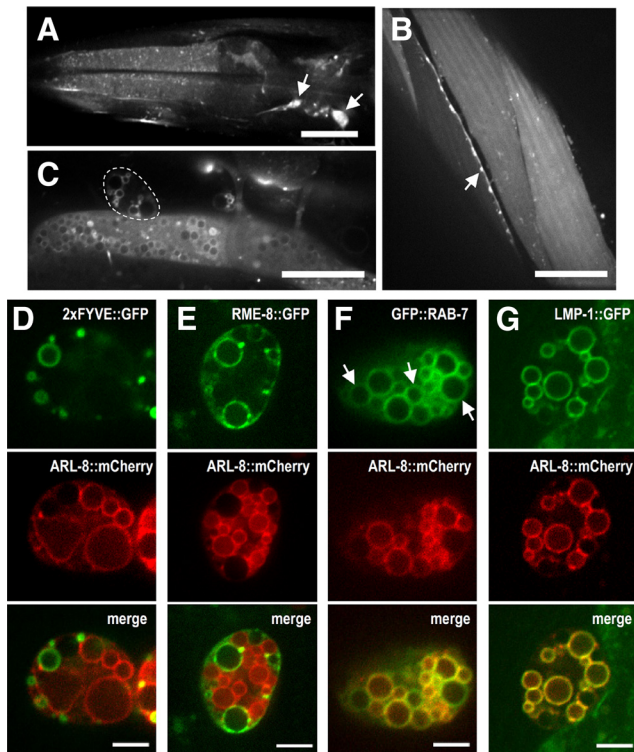


Figure 1. Expression and subcellular localization of fluorescent protein-tagged ARL-8 in worm tissues. (A–C) Expression of ARL-8::GFP driven by the *arl-8* promoter in live adult worms. Expression was observed in the pharynx (A), muscle (B), neurons (arrows in A and B), intestine (C), and coelomocytes. A coelomocyte is delineated by a dashed line in C. Bars, 20 μ m. (D–G) Analysis of subcellular localization of ARL-8::mCherry in coelomocytes expressing the indicated GFP fusion markers of early endosomes (2xFYVE::GFP; D), early/late endosomes (RME-8::GFP; E), late endosomes/lysosomes (GFP::RAB-7; F), and lysosomes (LMP-1::GFP; G). ARL-8::mCherry was localized to membrane compartments, which were not labeled with 2xFYVE::GFP or RME-8::GFP, but with GFP::RAB-7 and LMP-1::GFP. Some GFP::RAB-7-labeled compartments were negative for ARL-8::mCherry (arrows in F), whereas essentially all LMP-1::GFP-labeled compartments were positive for ARL-8::mCherry. Bars, 5 μ m.

tion of ARL-8 in coelomocytes, we performed double labeling of ARL-8::mCherry with endocytic compartment GFP markers. ARL-8::mCherry did not overlap with 2xFYVE::GFP (early endosomes; Nicot *et al.*, 2006) or RME-8::GFP (early/late endosomes; Zhang *et al.*, 2001; Figure 1, D and E). In contrast, most ARL-8::mCherry colocalized well with GFP::RAB-7 (late endosomes/lysosomes; Poteryaev *et al.*, 2007) and LMP-1::GFP (lysosomes; Treusch *et al.*, 2004; Figure 1, F and G). More precisely, ARL-8::mCherry showed virtually complete overlap with LMP-1::GFP, whereas there were some GFP::RAB-7-positive compartments lacking ARL-8::mCherry (arrows in Figure 1F). These results indicate that, as the mammalian counterpart, *C. elegans* Arl8 localizes primarily to lysosomes.

ARL-8 Is Required Maternally for Embryonic Development

To investigate the physiological role of ARL-8 *in vivo*, we isolated a mutant carrying a deletion in the *arl-8* gene, *arl-8(tm2504)*. Western blot analysis using an anti-ARL-8 antibody indicates that the deletion is a strong loss-of-function or null mutation (Supplemental Figure S1). Animals heterozygous for *arl-8(tm2504)* displayed no observable phenotype and were

mainly used as control animals in this study. Homozygous *arl-8* animals from heterozygous *arl-8(tm2504)* mothers developed to fertile adults; however, no viable embryos were produced by hermaphrodites homozygous for *arl-8(tm2504)*, suggesting that ARL-8 is required maternally for embryonic development (not shown). The embryonic lethality was efficiently rescued by introduction of wild-type *arl-8* (*arl-8/WT*) or a constitutively active mutant (*arl-8/Q75L*) but not by a putative nucleotide-free mutant (*arl-8/T34N*), suggesting that function of ARL-8 as a guanine nucleotide-binding protein is important for normal embryogenesis (Supplemental Figure S1). Furthermore, expression of human Arl8 proteins in *arl-8* mutants could also rescue the embryonic lethality, indicating that Arl8 plays a conserved role in multicellular animals. The basis of the embryonic lethality is under investigation and we focus on the coelomocyte phenotypes in this study.

arl-8 Mutant Coelomocytes Display Supernumerary Late Endosomal and Lysosomal Compartments That Are Smaller than Wild Type

Figure 2A shows the localization of endocytic compartment markers in *arl-8(tm2504)* coelomocytes. The morphologies of 2xFYVE- and RME-8-positive compartments in *arl-8(tm2504)* coelomocytes were indistinguishable from those in control ones. In contrast, the *arl-8(tm2504)* mutation caused an increase in the number of RAB-7- or LMP-1-positive compartments, most of which were smaller in size compared with those of control animals (Figure 2, B and C). These data suggest that the morphologies of late endosomes/lysosomes, but not early endocytic organelles, are specifically affected in *arl-8(tm2504)* coelomocytes. To test if the increased number of RAB-7- or LMP-1-positive compartments reflected an increase in concentration of RAB-7 or LMP-1, we quantified fluorescence intensities of GFP::RAB-7 in coelomocytes and found that GFP::RAB-7 levels were not increased but rather reduced slightly in *arl-8* mutant coelomocytes than those in control (Supplemental Figure S2).

The aberrant morphologies of RAB-7- or LMP-1-positive compartments in *arl-8* mutant coelomocytes were not so obvious until adult stage (not shown), raising the possibility that progressive developmental abnormalities in *arl-8* mutants irreversibly impaired their morphologies in coelomocytes. Thus, we examined whether heat-shock promoter-driven expression of *arl-8* in adult stages of *arl-8* mutants can rescue the phenotypes. We found a decrease in the abnormal size and number of those organelles in the mutant after a brief heat shock compared with siblings that did not have heat-shock-induced expression of ARL-8::mCherry (Figure 2D). These results indicate that the morphologies of RAB-7- or LMP-1-positive compartments are not irreversibly impaired in adult *arl-8* mutants but can be restored upon *arl-8* expression.

Formation of the Supernumerary Membrane Compartments in *arl-8* Mutants Is Largely Suppressed by Blocking Early-to-Late Endosomal Traffic

To test if endocytic membrane traffic is involved in formation of the supernumerary membrane compartments in *arl-8* mutants, we analyzed a genetic interaction of *arl-8* with *sand-1*, which is required for early-to-late endosomal traffic (Poteryaev *et al.*, 2007). In *sand-1* mutants, no or little endocytosed macromolecules exit from early endosomes, which results in accumulation of endocytic contents in enlarged endosomes (Poteryaev *et al.*, 2007). Indeed, RNAi against *sand-1* induced enlarged RME-8-labeled endosomes with no apparent changes in 2xFYVE-labeled endosomes (Supplemental Figure S3). We found that formation of supernumerary LMP-1-labeled compartments in *arl-8* mutants was largely suppressed

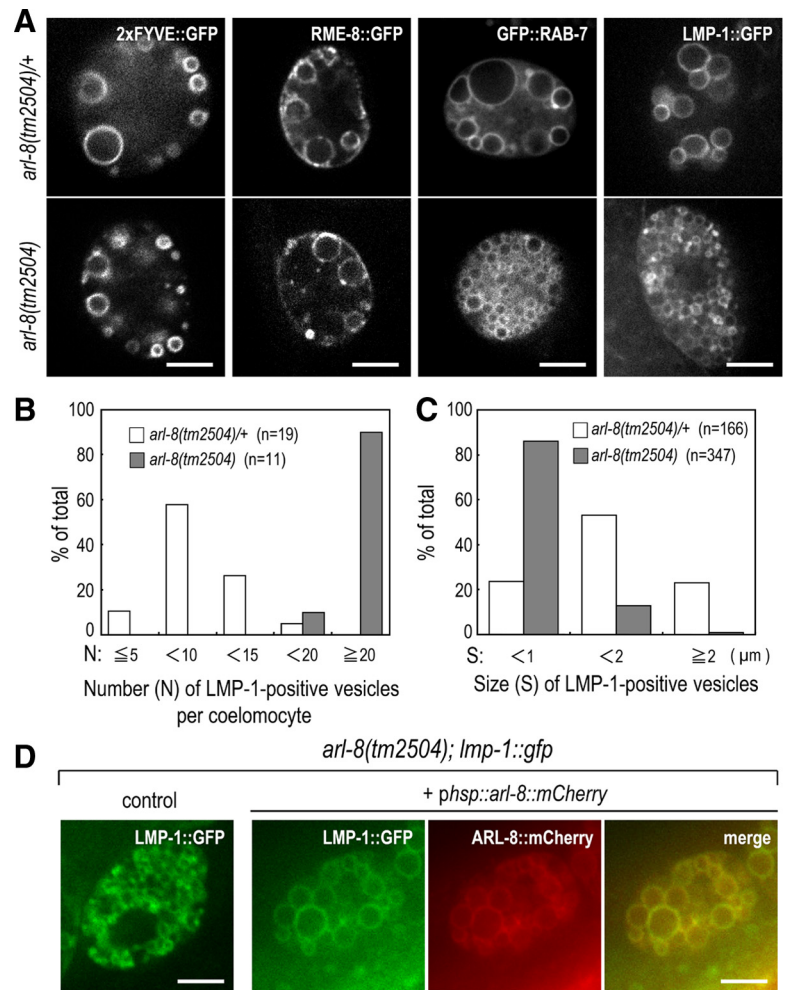


Figure 2. *arl-8(tm2504)* coelomocytes display supernumerary RAB-7- and LMP-1-positive compartments that are smaller than wild type. (A) Confocal images of *arl-8(tm2504)/+* and *arl-8(tm2504)* coelomocytes expressing the indicated GFP-fusion markers. *tm2504* mutation resulted in a decrease in the sizes of the RAB-7- and LMP-1-positive compartments with increase in the number of these compartments. (B and C) Quantification of the number and size of LMP-1-positive compartments in *arl-8(tm2504)/+* and *arl-8(tm2504)* coelomocytes. LMP-1-positive compartments were scored at a single focal plane and sorted into five and three categories according to their number and size, respectively. (D) Rescue of the aberrant morphologies of LMP-1-positive compartments in *arl-8* mutants by expression of ARL-8::mCherry under the heat-shock promoters. Adult *arl-8* mutants expressing LMP-1::GFP with or without extrachromosomal arrays of *phsp::arl-8::mCherry* were heat-shocked and observed 24 h after heat shock. Bars, 5 μm.

by *sand-1(RNAi)* (Figure 3), suggesting that the majority of the supernumerary membrane compartments in *arl-8* mutants are late endosomal compartments generated via early-to-late endosomal traffic.

Transport of Endocytosed Macromolecules to ASP-1-enriched Lysosomal Compartments Is Impaired in *arl-8* Mutants

We next analyzed endocytic traffic in *arl-8* mutant coelomocytes. Coelomocytes actively take up endocytosis markers

such as fluorescently labeled proteins that are delivered into the pseudocoelom (body cavity) by transgene expression or microinjection (Fares and Greenwald, 2001a). Previous studies have shown that TR-BSA injected into the pseudocoelom travels through the RME-8-labeled compartments and finally reaches the LMP-1-labeled compartments in wild-type coelomocytes (Zhang *et al.*, 2001; Treusch *et al.*, 2004; Gengyo-Ando *et al.*, 2007; Poteryaev *et al.*, 2007). To analyze early endocytic trafficking in *arl-8(tm2504)* coelomocytes, we injected TR-BSA into animals expressing RME-8::GFP in

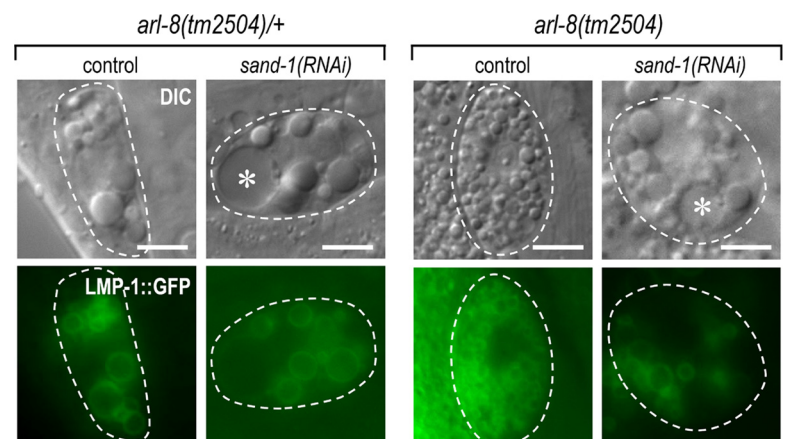


Figure 3. *sand-1(RNAi)* suppresses the formation of supernumerary LMP-1-positive membrane compartments in *arl-8* mutants. Nomarski and fluorescence images of LMP-1::GFP-expressing coelomocytes of the *arl-8(tm2504)/+*, *arl-8(tm2504)/+;sand-1(RNAi)*, *arl-8(tm2504)*, or *arl-8(tm2504);sand-1(RNAi)*. Asterisks show enlarged endosomes. Bars, 5 μm.

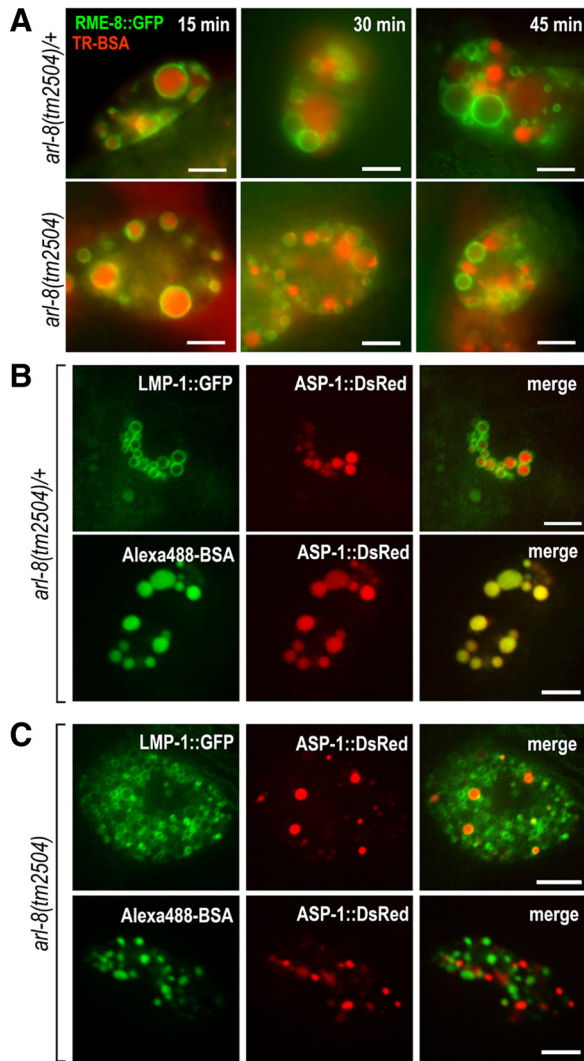


Figure 4. (A) Time-course analysis of endocytic trafficking of TR-BSA in *arl-8(tm2504)/+* and *arl-8(tm2504)* coelomocytes expressing RME-8::GFP. Shown are fluorescence images of the coelomocytes at the indicated time after injection of TR-BSA into the body cavity of the respective worms. (B and C) Endocytosed macromolecules fail to reach ASP-1-enriched compartments in *arl-8(tm2504)* coelomocytes. Shown are confocal images of the coelomocytes in the respective worms coexpressing LMP-1::GFP and ASP-1::DsRed (top panels in B and C) or confocal images of the coelomocytes 3.5 h after injection of Alexa488-BSA into the body cavity of the respective worms expressing ASP-1::DsRed (bottom panels in B and C). Bars, 5 μm.

coelomocytes. Figure 4A shows that the endocytosed TR-BSA accumulated in the RME-8::GFP-positive compartments within 15 min after injection and then appeared in distinct compartments negative for RME-8::GFP in both control and *arl-8(tm2504)* coelomocytes by 45 min, indicating that early endocytic traffic is almost normal in *arl-8* mutants.

We next investigated late endocytic trafficking in *arl-8(tm2504)* coelomocytes. ASP-1 is a *C. elegans* aspartic protease, which is homologous to human lysosomal enzyme cathepsin D (Tcherepanova *et al.*, 2000). In control coelomocytes, ASP-1::DsRed localized to virtually all of LMP-1-positive compartments (Figure 4B, top panel). After leaving RME-8-positive compartments, endocytosed macromole-

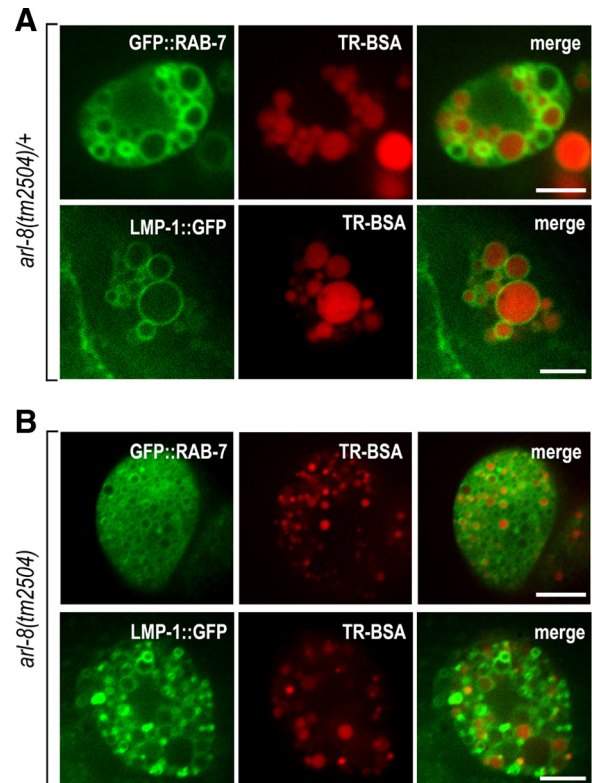


Figure 5. Localization of endocytosed TR-BSA in *arl-8(tm2504)/+* (A) or *arl-8(tm2504)* (B) coelomocytes expressing GFP::RAB-7 or LMP-1::GFP. Shown are confocal images of the coelomocytes 3.5 h after injection of TR-BSA into the body cavity of the respective worms. Bars, 5 μm.

cules were transported to RAB-7-positive/ASP-1-negative compartments and then reach to ASP-1-enriched compartments in control animals (Figure 4B, bottom panels, and Supplemental Figure S4), which appears to represent transport from late endosomes to lysosomes. In *arl-8* mutants, ASP-1 localized to LMP-1-positive compartments as in control coelomocytes; however, there were number of LMP-1-positive compartments with no or little ASP-1 (Figure 4C, top panels). Interestingly, endocytosed Alexa488-BSA failed to reach to ASP-1-enriched compartments in *arl-8* mutants (Figure 4C, bottom panels). In control coelomocytes, endocytosed TR-BSA was finally transported to most of RAB-7- or LMP-1-positive compartments, whereas it localized to a subpopulation of those compartments in *arl-8* mutants (Figure 5, A and B). Collectively, these results suggest that endocytosed macromolecules are delivered to RAB-7/LMP-1-positive late endosomal compartments in *arl-8* mutants; however, transport from those compartments to lysosomes is compromised.

Time-Lapse Analysis of Endocytic Traffic in Coelomocytes

To analyze the dynamics of endocytic traffic in coelomocytes, we developed a method for time-lapse imaging of isolated coelomocytes from adult animals. We applied Alexa488-BSA to the extracellular medium and recorded the endocytic traffic of Alexa488-BSA to ASP-1-positive compartments in wild-type coelomocytes. Endocytosed Alexa488-BSA accumulated in small compartments outside ASP-1-positive compartments at early time point and then underwent complete fusion with ASP-1-positive

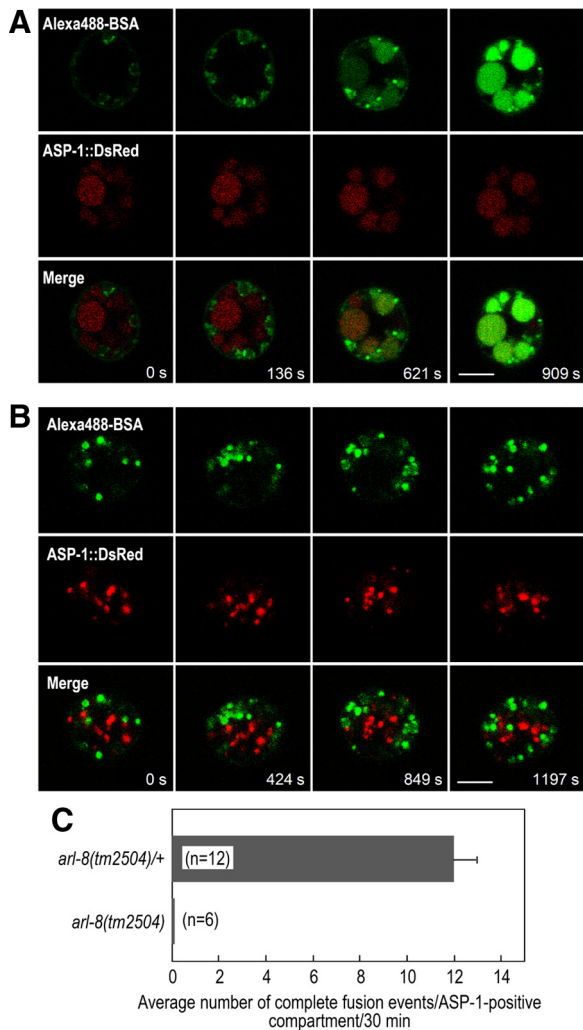


Figure 6. Time-lapse analysis of endocytic trafficking in coelomocytes. (A and B) Endocytic traffic of Alexa488-BSA to ASP-1-positive compartments in a control (A) or *arl-8(tm2504)* (B) coelomocyte. Pictures in A and B were extracted from Supplemental Movies 1 and 3, respectively. Bars, 5 μ m. (C) Quantitation of fusion events. Average numbers of Alexa488-BSA-containing compartments that fused with a single ASP-1-positive compartment for 30 min were determined in *arl-8(tm2504)/+* (n = 12) and *arl-8(tm2504)* (n = 6) coelomocytes. Error bar, SEM.

compartments, leading to the increase in Alexa488-fluorescence in the ASP-1-positive compartments (Figure 6A, Supplemental Figure S5, and Supplemental Movies 1 and 2). In *arl-8* mutants, endocytic compartments concentrating Alexa488-BSA were formed and occasionally contacted with ASP-1-positive compartments as in wild type. Only a small fraction of the interaction events led to appearance of Alexa488-BSA in ASP-1-positive compartments (Supplemental Figure S6); however, no apparent complete fusion between these two compartments was observed during the time courses of our live cell imaging (Figure 6B and Supplemental Movie 3). Quantitative analysis of fusion events revealed that the frequency of complete fusion between these compartments was greatly decreased in *arl-8* mutants (Figure 6C), suggesting that *arl-8* mutants have a defect in fusion between the Alexa488-BSA-containing compartments and ASP-1-positive compartments.

Transient Expression of *arl-8* Promotes the Formation of Alexa488-BSA and ASP-1::mCherry Double-positive Compartments in *arl-8* Mutants

We next investigated whether transient expression of *arl-8* can promote fusion between Alexa488-BSA-containing compartments and ASP-1-positive compartments in *arl-8* mutants. *arl-8* was expressed under heat-shock promoter in *arl-8(tm2504)* mutant coelomocytes where Alexa488-BSA and ASP-1::mCherry had been localized to distinct compartments before heat shock. We found that Alexa488-BSA and ASP-1::mCherry double-positive compartments were formed within 1 h after brief heat shock, and the population of those compartments was increased time-dependently in *arl-8* mutants harboring the transgene for heat shock-inducible expression of *arl-8* (Figure 7, A and B). Such a phenotype was never observed in siblings without the transgene. These results suggest that *arl-8* is involved in promotion of fusion between Alexa488-BSA-containing compartments and ASP-1-positive compartments.

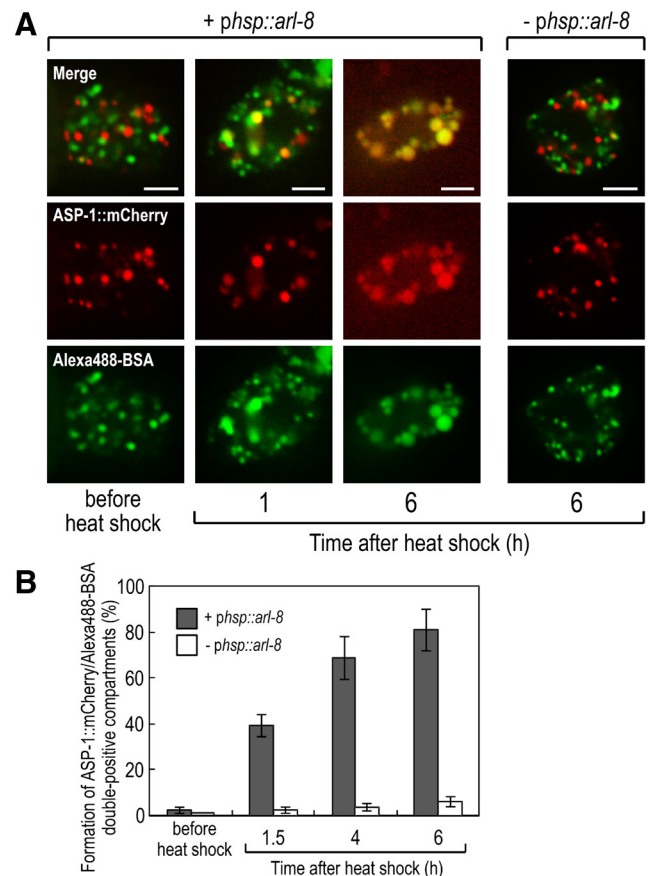


Figure 7. Transient expression of *arl-8* promotes the formation of Alexa488-BSA and ASP-1::mCherry double-positive compartments in *arl-8* mutants. (A) Alexa488-BSA was injected to ASP-1::mCherry-expressing *arl-8* mutants with or without extrachromosomal arrays of *phsp::arl-8* transgene and then incubated at 15°C for 15 h before heat shock at 33°C for 30 min. Shown are confocal images of the coelomocytes before heat shock or at the indicated times after heat shock. (B) The formation of Alexa488-BSA and ASP-1::mCherry double-positive compartments was quantified as the percentage of those compartments relative to the total number of Alexa488-BSA-containing compartments in *arl-8* mutant coelomocytes (n > 15) with or without extrachromosomal arrays of *phsp::arl-8* transgene. Error bars, SEM.

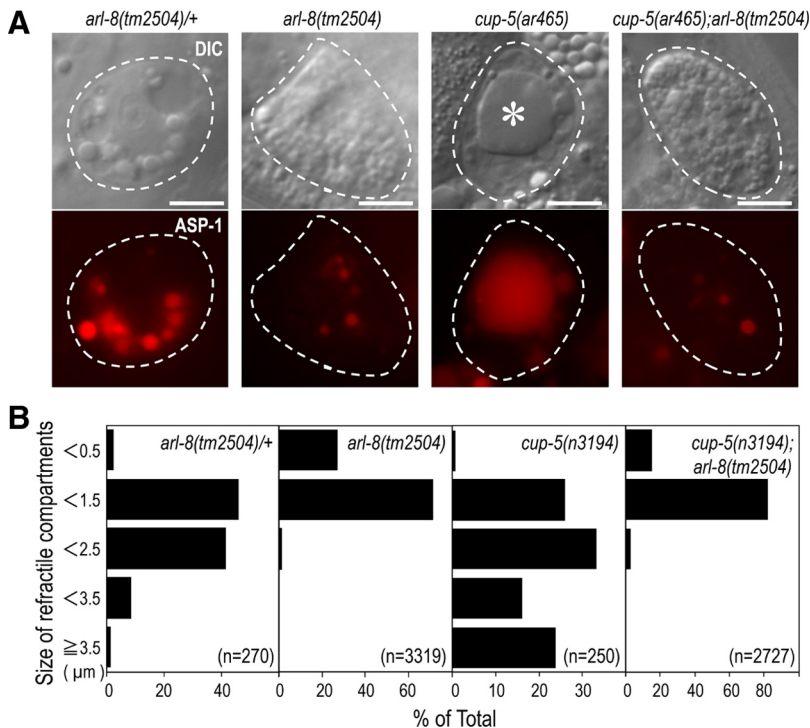


Figure 8. *arl-8* functions upstream to *cup-5*. (A) Nomarski and fluorescence images of the coelomocyte expressing ASP-1::dsRed or ASP-1::mCherry of the *arl-8(tm2504)/+*, *arl-8(tm2504)*, *cup-5(ar465)*, or *cup-5(ar465);arl-8(tm2504)*. An asterisk shows an aberrantly enlarged vacuole filled with ASP-1::mCherry in the *cup-5(ar465)* coelomocytes. Formation of the enlarged vacuoles is strongly suppressed in the *cup-5(ar465);arl-8(tm2504)* coelomocytes. (B) Quantification of refractile compartments of coelomocytes. Refractile compartments were scored at a single focal plane and sorted into five categories according to their size. Twenty to 25 coelomocytes were scored for each allele. Bars, 5 μm.

arl-8 Functions Upstream to *cup-5*

Recent studies have shown that delivery of endocytosed macromolecules to lysosomes is mediated by fusion between late endosomes and lysosomes (Luzio *et al.*, 2007). Late endosomes fuse with lysosomes to form hybrid organelles, from which lysosomes can be reformed via fission. We investigated a genetic interaction of *arl-8* with *cup-5*, which is involved in reformation of lysosomes from late endosome-lysosome hybrid organelles (Fares and Greenwald, 2001b; Hersh *et al.*, 2002). *cup-5* is the *C. elegans* orthologue of human mucolipin-1 implicated in mucopolipidosis type IV. *cup-5* mutant coelomocytes display enlarged vacuoles with properties of late endosome-lysosome hybrid organelles due to a defect in the reformation of lysosomes from the hybrid organelles (Piper and Luzio, 2004; Treusch *et al.*, 2004). If *arl-8* would promote fusion between late endosomes and lysosomes, *arl-8* would be required for formation of the enlarged vacuoles in *cup-5* mutants. Consistent with this prediction, formation of the enlarged vacuoles of *cup-5(ar465)* mutants was strongly suppressed by the *arl-8(tm2504)* mutation (Figure 8A). The same results were obtained using the *cup-5* null allele *n3194*, the quantification of which is shown in Figure 8B. ASP-1::mCherry localized primarily to enlarged vacuoles in *cup-5* mutants, whereas it localized to a subpopulation of small compartments in *cup-5; arl-8* mutant coelomocytes as observed in *arl-8* mutants. These results are consistent with the idea that ARL-8 facilitates late endosome-lysosome fusion.

DISCUSSION

In the present study, we have shown that *arl-8(tm2504)* mutants display the unique late endosomal/lysosomal phenotypes that are unprecedented in previous studies: Loss of *arl-8* resulted in supernumerary late endosomal and lysosomal compartments that were smaller than wild type. Formation of the supernumerary compartments was largely suppressed by blocking of early-to-late endosomal traffic using

sand-1(RNAi). Endocytosed macromolecules were transported to late endosomal compartments in *arl-8* mutants; however, the compartments fail to fuse with ASP-1-enriched lysosomal compartments. Finally, loss-of-function of ARL-8 suppresses the enlargement of late endosome-lysosome hybrid organelles caused by mutations of *cup-5*. A proposed model of endocytic pathway in coelomocytes is shown in Supplemental Figure S7.

There is now compelling evidence that the transport of endocytosed macromolecules to lysosomes is mediated by fusion between late endosomes and lysosomes (Futter *et al.*, 1996; Bright *et al.*, 1997; Mullock *et al.*, 1998; Pryor *et al.*, 2000; Ward *et al.*, 2000; Bright *et al.*, 2005). We have shown that endocytosed Alexa488-BSA-containing compartments completely fused with ASP-1-enriched compartments in wild-type coelomocyte, which may correspond to late endosome-lysosome fusion in mammalian cells. In *arl-8* mutants, endocytosed macromolecules were transported to RAB-7-positive/ASP-1-negative compartments as in wild-type coelomocytes; however, these compartments failed to undergo complete fusion with ASP-1-enriched compartments, suggesting a defect in fusion between late endosomes and lysosomes in *arl-8* mutants. It should be noted that RAB-7-positive/ASP-1-negative compartments, where endocytosed macromolecules were transported, were positive also for LMP-1 in *arl-8* mutants, whereas those of wild-type had no or little LMP-1 (not shown). Late endosomal compartments in *arl-8* mutants may thus have distinct properties from those in wild type, although we cannot rule out the possibility of transient localization of LMP-1 to RAB-7-positive/ASP-1-negative compartments in wild-type coelomocytes.

How could ARL-8 regulate fusion between late endosomes and lysosomes? ARL-8 may indirectly regulate SNARE function required for late endosome-lysosome fusion through effector molecules in a similar manner to those observed for Rab GTPases (Grosshans *et al.*, 2006). Interaction of the Rab5 effector EEA1 (a coiled-coil tethering factor) with syntaxin-13

(t-SNARE) is required for homotypic early endosome fusion. The class C-VPS/HOPS tethering complex, an effector of the yeast Rab Ypt7p, binds SNAREs required for vacuole fusion. Alternatively, given that mammalian Arl8 has been shown to be involved in a microtubule-dependent lysosomal transport (Bagshaw *et al.*, 2006; Hofmann and Munro, 2006), ARL-8 may promote late endosome-lysosome fusion by regulating lysosome motility along microtubules. Indeed, Rab GTPases orchestrate membrane fusion not only by recruiting the components of the fusion machinery, but also by controlling motor-based vesicle transport (Jordens *et al.*, 2005). Interaction of Rab5 with Vps34 leads to local early endosomal production of phosphatidylinositol-3-phosphate, which not only attracts EEA1 but also recruits KIF16B (a PX-domain containing kinesin), thereby stimulating plus-end transport of the endosomes (Hoepfner *et al.*, 2005). Rab7 also regulates dynein/dynactin-motor recruitment to late endosomes via interaction with the two effectors, RILP and ORP1L (Johansson *et al.*, 2007). Although ARL-8/Arl8 localizes primarily to lysosomes in *C. elegans* coelomocytes/mammalian cells, we cannot rule out the possibility that loss of *arl-8* affects late endosomal biogenesis and/or functions critical for fusion with lysosomes because late endosome morphologies appear to be affected in *arl-8* mutants. Understanding the molecular event in late endosome-lysosome system that involves ARL-8 requires identification of effectors and other interacting proteins for ARL-8.

Late endosome-lysosome fusion mediates transport of newly synthesized lysosomal enzymes to lysosomes in mammalian cells (Luzio *et al.*, 2003). Besides complete fusion, transient fusion between late endosomes and lysosomes (“kiss-and-run”) has also been shown to mediate endocytic delivery to lysosomes in mammalian cells (Bright *et al.*, 2005). Considering that transient fusion, together with complete fusion, was rarely observed in *arl-8* mutants, there appears to be little, if any, contribution of these fusion events to transport of ASP-1 to LMP-1-positive compartments in *arl-8* mutants. ASP-1 may be transported directly to LMP-1-positive lysosomes in a similar manner to the yeast ALP pathway, in which hydrolytic enzymes bypass endosomes and reach directly to the vacuoles, the equivalent of the mammalian lysosome (Cowles *et al.*, 1997; Piper *et al.*, 1997; Stepp *et al.*, 1997).

We previously reported that mammalian Arl8 localized to spindle midbody in mitotic PC12 cells, together with perinuclear localization in the interphase cells and that Arl8 may be involved in chromosome segregation in cultured mammalian and fly cells (Okai *et al.*, 2004). No apparent mitotic spindle localization of Arl8 was, however, observed in most mammalian cell lines other than PC12 cells we tested, and no apparent defect in chromosome segregation was detected in *arl-8(tm2504)* mutant embryos (not shown). Arl8 is thus not likely to make significant contribution to chromosome segregation in most cell types, although we cannot rule out the possibility that Arl8 have a role in the mitotic spindle of certain cell types and/or under some circumstances.

Besides the late endosomal-lysosomal system, what cellular processes would *arl-8* be involved in? Considering that phagosome-lysosome fusion contributes to the removal of apoptotic cells during programmed cell death in *C. elegans* (Kinchen *et al.*, 2008; Lu *et al.*, 2008; Mangahas *et al.*, 2008; Xiao *et al.*, 2009), *arl-8* may function in clearance of apoptotic cells. In *C. elegans* embryos, ARL-8 may be localized to lysosome-related yolk granules and involved in the degradation of yolk proteins, which are important sources of nutrition and energy during embryogenesis (Fagotto, 1995). Lysosome-related organelles such as yolk granules are a group of cell type-specific compartments that share various features with lysosomes, but are distinct in function, morphology, and composition (Dell’Angelica *et al.*,

2000). Gut granules are also intestine-specific lysosome-related organelles in *C. elegans* (Hermann *et al.*, 2005). In mammals, lysosome-related organelles include melanosomes, lytic granules, major histocompatibility complex class II compartments, platelet-dense granules, basophil granules, and neutrophil azurophil granules. Given that recent organelle proteomics studies in mammals have revealed that Arl8 is detected in some lysosome-related organelles (Bagshaw *et al.*, 2005; Hu *et al.*, 2007), this GTPase may also be crucial for the biogenesis and functions of these lysosome-related organelles.

ACKNOWLEDGMENTS

We gratefully acknowledge B. Grant (Department of Molecular Biology and Biochemistry, Rutgers University) for the RME-8::GFP-expressing strain and R. Y. Tsien (HHMI, University of California, San Diego) for mCherry plasmids. J. Rothman and E. Witze for providing insightful and invaluable comments on this manuscript. E. Kuranaga and Tokyo University Leica Imaging Center for expert technical assistance of time-lapse analysis, and present and former members of the Katada laboratory for useful discussions. Some *C. elegans* stains used in this study were provided by the *Caenorhabditis* Genetics Center, which is funded by the National Institutes of Health National Center for Research Resources. This work was supported in part by research grants from the Ministry of Education, Culture, Sports, Science, and Technology (MEXT) of Japan (K.K., T.K., K.G.-A., and S.M.), Japan Society for the Promotion of Science (JSPS; K.K., T.K., K.G.-A., and S.M.), and Japan Science and Technology Agency (JST; K.G.-A. and S.M.).

REFERENCES

- Bagshaw, R. D., Callahan, J. W., and Mahuran, D. J. (2006). The Arf-family protein, Arl8b, is involved in the spatial distribution of lysosomes. *Biochem. Biophys. Res. Commun.* 344, 1186–1191.
- Bagshaw, R. D., Mahuran, D. J., and Callahan, J. W. (2005). A proteomic analysis of lysosomal integral membrane proteins reveals the diverse composition of the organelle. *Mol. Cell Proteom.* 4, 133–143.
- Brenner, S. (1974). The genetics of *Caenorhabditis elegans*. *Genetics* 77, 71–94.
- Bright, N. A., Gratian, M. J., and Luzio, J. P. (2005). Endocytic delivery to lysosomes mediated by concurrent fusion and kissing events in living cells. *Curr. Biol.* 15, 360–365.
- Bright, N. A., Reaves, B. J., Mullock, B. M., and Luzio, J. P. (1997). Dense core lysosomes can fuse with late endosomes and are re-formed from the resultant hybrid organelles. *J. Cell Sci.* 110(Pt 17), 2027–2040.
- Cowles, C. R., Snyder, W. B., Burd, C. G., and Emr, S. D. (1997). Novel Golgi to vacuole delivery pathway in yeast: identification of a sorting determinant and required transport component. *EMBO J.* 16, 2769–2782.
- Dell’Angelica, E. C., Mullins, C., Caplan, S., and Bonifacino, J. S. (2000). Lysosome-related organelles. *FASEB J.* 14, 1265–1278.
- Espelt, M. V., Estevez, A. Y., Yin, X., and Strange, K. (2005). Oscillatory Ca²⁺ signaling in the isolated *Caenorhabditis elegans* intestine: role of the inositol-1,4,5-trisphosphate receptor and phospholipases C beta and gamma. *J. Gen. Physiol.* 126, 379–392.
- Fagotto, F. (1995). Regulation of yolk degradation, or how to make sleepy lysosomes. *J. Cell Sci.* 108(Pt 12), 3645–3647.
- Fares, H., and Greenwald, I. (2001a). Genetic analysis of endocytosis in *Caenorhabditis elegans*: coelomocyte uptake defective mutants. *Genetics* 159, 133–145.
- Fares, H., and Greenwald, I. (2001b). Regulation of endocytosis by CUP-5, the *Caenorhabditis elegans* mucolipin-1 homolog. *Nat. Genet.* 28, 64–68.
- Futter, C. E., Pearse, A., Hewlett, L. J., and Hopkins, C. R. (1996). Multivesicular endosomes containing internalized EGF-EGF receptor complexes mature and then fuse directly with lysosomes. *J. Cell Biol.* 132, 1011–1023.
- Gengyo-Ando, K., Kuroyanagi, H., Kobayashi, T., Murate, M., Fujimoto, K., Okabe, S., and Mitani, S. (2007). The SM protein VPS-45 is required for RAB-5-dependent endocytic transport in *Caenorhabditis elegans*. *EMBO Rep.* 8, 152–157.
- Gengyo-Ando, K., and Mitani, S. (2000). Characterization of mutations induced by ethyl methanesulfonate, UV, and trimethylpsoralen in the nematode *Caenorhabditis elegans*. *Biochem. Biophys. Res. Commun.* 269, 64–69.
- Gengyo-Ando, K., Yoshina, S., Inoue, H., and Mitani, S. (2006). An efficient transgenic system by TA cloning vectors and RNAi for *C. elegans*. *Biochem. Biophys. Res. Commun.* 349, 1345–1350.

- Gillingham, A. K., and Munro, S. (2007). The small G proteins of the Arf family and their regulators. *Annu. Rev. Cell Dev. Biol.* 23, 579–611.
- Grant, B. D., and Sato, M. Intracellular trafficking (January 21, 2006) WormBook, ed. The *C. elegans* Research Community, WormBook, doi/10.1895/wormbook.1.77.1, http://www.wormbook.org.
- Grosshans, B. L., Ortiz, D., and Novick, P. (2006). Rabs and their effectors: achieving specificity in membrane traffic. *Proc. Natl. Acad. Sci. USA.* 103, 11821–11827.
- Hermann, G. J., Schroeder, L. K., Hieb, C. A., Kershner, A. M., Rabbitts, B. M., Fonarev, P., Grant, B. D., and Priess, J. R. (2005). Genetic analysis of lysosomal trafficking in *Caenorhabditis elegans*. *Mol. Biol. Cell* 16, 3273–3288.
- Hersh, B. M., Hartwig, E., and Horvitz, H. R. (2002). The *Caenorhabditis elegans* mucopolipin-like gene cup-5 is essential for viability and regulates lysosomes in multiple cell types. *Proc. Natl. Acad. Sci. USA.* 99, 4355–4360.
- Hoepfner, S., Severin, F., Cabezas, A., Habermann, B., Runge, A., Gillyooly, D., Stenmark, H., and Zerial, M. (2005). Modulation of receptor recycling and degradation by the endosomal kinesin KIF16B. *Cell* 121, 437–450.
- Hofmann, I., and Munro, S. (2006). An N-terminally acetylated Arf-like GTPase is localised to lysosomes and affects their motility. *J. Cell Sci.* 119, 1494–1503.
- Hu, Z. Z., Valencia, J. C., Huang, H., Chi, A., Shabanowitz, J., Hearing, V. J., Appella, E., and Wu, C. (2007). Comparative bioinformatics analyses and profiling of lysosome-related organelle proteomes. *Int. J. Mass Spectrom* 259, 147–160.
- Johansson, M., Rocha, N., Zwart, W., Jordens, I., Janssen, L., Kuijl, C., Olkkonen, V. M., and Neeffes, J. (2007). Activation of endosomal dynein motors by stepwise assembly of Rab7-RILP-p150Glued, ORP1L, and the receptor betall spectrin. *J. Cell Biol.* 176, 459–471.
- Jordens, I., Marsman, M., Kuijl, C., and Neeffes, J. (2005). Rab proteins, connecting transport and vesicle fusion. *Traffic* 6, 1070–1077.
- Kahn, R. A., Volpicelli-Daley, L., Bowzard, B., Shrivastava-Ranjan, P., Li, Y., Zhou, C., and Cunningham, L. (2005). Arf family GTPases: roles in membrane traffic and microtubule dynamics. *Biochem. Soc. Trans.* 33, 1269–1272.
- Kajiho, H., Saito, K., Tsujita, K., Kontani, K., Araki, Y., Kurosu, H., and Katada, T. (2003). RIN3, a novel Rab5 GEF interacting with amphiphysin II involved in the early endocytic pathway. *J. Cell Sci.* 116, 4159–4168.
- Kamath, R. S., Martinez-Campos, M., Zipperlen, P., Fraser, A. G., and Ahringer, J. (2001). Effectiveness of specific RNA-mediated interference through ingested double-stranded RNA in *Caenorhabditis elegans*. *Genome. Biol.* 2, RESEARCH0002.
- Kinchen, J. M., Doukoumetzidis, K., Almendinger, J., Stergiou, L., Tosello-Tramont, A., Sifri, C. D., Hengartner, M. O., and Ravichandran, K. S. (2008). A pathway for phagosome maturation during engulfment of apoptotic cells. *Nat. Cell Biol.* 10, 556–566.
- Li, Y., Kelly, W. G., Logsdon, J. M., Jr., Schurko, A. M., Harfe, B. D., Hill-Harfe, K. L., and Kahn, R. A. (2004). Functional genomic analysis of the ADP-ribosylation factor family of GTPases: phylogeny among diverse eukaryotes and function in *C. elegans*. *FASEB J.* 18, 1834–1850.
- Lu, Q., Zhang, Y., Hu, T., Guo, P., Li, W., and Wang, X. (2008). *C. elegans* Rab GTPase 2 is required for the degradation of apoptotic cells. *Development* 135, 1069–1080.
- Luzio, J. P., Poupon, V., Lindsay, M. R., Mullock, B. M., Piper, R. C., and Pryor, P. R. (2003). Membrane dynamics and the biogenesis of lysosomes. *Mol. Membr. Biol.* 20, 141–154.
- Luzio, J. P., Pryor, P. R., and Bright, N. A. (2007). Lysosomes: fusion and function. *Nat. Rev. Mol. Cell Biol.* 8, 622–632.
- Mangahas, P. M., Yu, X., Miller, K. G., and Zhou, Z. (2008). The small GTPase Rab2 functions in the removal of apoptotic cells in *Caenorhabditis elegans*. *J. Cell Biol.* 180, 357–373.
- Mello, C. C., Kramer, J. M., Stinchcomb, D., and Ambros, V. (1991). Efficient gene transfer in *C. elegans*: extrachromosomal maintenance and integration of transforming sequences. *EMBO J.* 10, 3959–3970.
- Mullins, C., and Bonifacino, J. S. (2001). The molecular machinery for lysosome biogenesis. *Bioessays* 23, 333–343.
- Mullock, B. M., Bright, N. A., Fearon, C. W., Gray, S. R., and Luzio, J. P. (1998). Fusion of lysosomes with late endosomes produces a hybrid organelle of intermediate density and is NSF dependent. *J. Cell Biol.* 140, 591–601.
- Nicot, A. S., Fares, H., Payrastra, B., Chisholm, A. D., Labouesse, M., and Laporte, J. (2006). The phosphoinositide kinase PIKfyve/Fab1p regulates terminal lysosome maturation in *Caenorhabditis elegans*. *Mol. Biol. Cell* 17, 3062–3074.
- Okai, T., Araki, Y., Tada, M., Tateno, T., Kontani, K., and Katada, T. (2004). Novel small GTPase subfamily capable of associating with tubulin is required for chromosome segregation. *J. Cell Sci.* 117, 4705–4715.
- Piper, R. C., Bryant, N. J., and Stevens, T. H. (1997). The membrane protein alkaline phosphatase is delivered to the vacuole by a route that is distinct from the VPS-dependent pathway. *J. Cell Biol.* 138, 531–545.
- Piper, R. C., and Luzio, J. P. (2004). CUPpling calcium to lysosomal biogenesis. *Trends Cell Biol.* 14, 471–473.
- Poteryaev, D., Fares, H., Bowerman, B., and Spang, A. (2007). *Caenorhabditis elegans* SAND-1 is essential for RAB-7 function in endosomal traffic. *EMBO J.* 26, 301–312.
- Pryor, P. R., Mullock, B. M., Bright, N. A., Gray, S. R., and Luzio, J. P. (2000). The role of intraorganellar Ca(2+) in late endosome-lysosome heterotypic fusion and in the reformation of lysosomes from hybrid organelles. *J. Cell Biol.* 149, 1053–1062.
- Saito, K., Murai, J., Kajiho, H., Kontani, K., Kurosu, H., and Katada, T. (2002). A novel binding protein composed of homophilic tetramer exhibits unique properties for the small GTPase Rab5. *J. Biol. Chem.* 277, 3412–3418.
- Stenmark, H. (2009). Rab GTPases as coordinators of vesicle traffic. *Nat. Rev. Mol. Cell Biol.* 10, 513–525.
- Stepp, J. D., Huang, K., and Lemmon, S. K. (1997). The yeast adaptor protein complex, AP-3, is essential for the efficient delivery of alkaline phosphatase by the alternate pathway to the vacuole. *J. Cell Biol.* 139, 1761–1774.
- Storrie, B., and Desjardins, M. (1996). The biogenesis of lysosomes: is it a kiss and run, continuous fusion and fission process? *Bioessays* 18, 895–903.
- Tcherepanova, I., Bhattacharyya, L., Rubin, C. S., and Freedman, J. H. (2000). Aspartic proteases from the nematode *Caenorhabditis elegans*. Structural organization and developmental and cell-specific expression of asp-1. *J. Biol. Chem.* 275, 26359–26369.
- Treusch, S., Knuth, S., Slaugenhaupt, S. A., Goldin, E., Grant, B. D., and Fares, H. (2004). *Caenorhabditis elegans* functional orthologue of human protein h-mucopolipin-1 is required for lysosome biogenesis. *Proc. Natl. Acad. Sci. USA.* 101, 4483–4488.
- Ward, D. M., Pevsner, J., Scullion, M. A., Vaughn, M., and Kaplan, J. (2000). Syntaxin 7 and VAMP-7 are soluble N-ethylmaleimide-sensitive factor attachment protein receptors required for late endosome-lysosome and homotypic lysosome fusion in alveolar macrophages. *Mol. Biol. Cell* 11, 2327–2333.
- Xiao, H., Chen, D., Fang, Z., Xu, J., Sun, X., Song, S., Liu, J., and Yang, C. (2009). Lysosome biogenesis mediated by vps-18 affects apoptotic cell degradation in *Caenorhabditis elegans*. *Mol. Biol. Cell* 20, 21–32.
- Zerial, M., and McBride, H. (2001). Rab proteins as membrane organizers. *Nat. Rev. Mol. Cell Biol.* 2, 107–117.
- Zhang, Y., Grant, B., and Hirsh, D. (2001). RME-8, a conserved J-domain protein, is required for endocytosis in *Caenorhabditis elegans*. *Mol. Biol. Cell* 12, 2011–2021.